

# A Message-Passing Approach for Joint Channel Estimation, Interference Mitigation and Decoding

Yan Zhu, Dongning Guo and Michael L. Honig

Department of Electrical Engineering and Computer Science

Northwestern University, Evanston, Illinois 60208

## Abstract

This paper studies receiver design for a wireless channel model with strong co-channel interference and fading. The time-varying channel gain of the desired signal can usually be measured through the use of pilots. We consider the case where no pilot for the interference signal is available for measuring its channel fading states. Because the interference process is often non-Gaussian, treating it as Gaussian noise may lead to poor performance, especially when it is as strong as the desired signal. For a Markov fading process, we propose an iterative message-passing architecture for joint channel estimation, interference and decoding. The associated belief propagation algorithm is capable of exploiting the statistics of the interference and correlated fading. Each message takes the form of a mixture of Gaussian densities where the number of components grows exponentially with the number of iterations. We limit the number of Gaussian components in each message so that the overall complexity of the receiver is constant per symbol regardless of the frame and code lengths. Simulation of both coded and uncoded systems shows that the receiver performs significantly better than conventional receivers with linear channel estimation.

## I. INTRODUCTION

Given a sufficient signal-to-noise ratio, the performance of a wireless terminal is fundamentally limited by two major factors, namely, interference from other terminals in the system and

This work was supported in part by the Northwestern Motorola Center for Seamless Communications.

uncertainty about channel variations. Although each of these two impairments has been studied in depth assuming the absence of the other, much less is understood when both are significant. This work considers the detection of one data signal in the presence of correlated fading and an interfering signal of the same modulation type, subject to independent correlated fading, and possibly of similar strength. Moreover, it is assumed that the channel condition of the desired user can be measured using known pilots interleaved with data symbols, whereas no pilot from the interferer is available at the receiver. Such a situation arises, for example, in peer-to-peer networks and in cellular networks with strong co-channel interference dominated by a signal from an adjacent cell.

This work focuses on a narrowband system with binary phase shift keying (BPSK) modulation, where the fading channels of the desired user and the interferer are modeled as independent Gauss-Markov processes.<sup>1</sup> In addition to its own applications, the model is the elementary building block for orthogonal frequency division multiplexing (OFDM). A single transmit antenna and dual receive antennas are assumed to develop the approach, although we also discuss extensions to more elaborate models.

The unique challenge posed by the model considered is the simultaneous uncertainty associated with the interference and fading channels. A conventional approach is to first measure the channel state (with or without interference), and then mitigate the interference assuming the channel estimate is exact. Such separation of channel estimation and detection is viable in the current problem if *known* pilots are also embedded in the interference. As was shown in [1], knowledge of pilots in the interfering signal can be indispensable to the success of linear channel estimation, even with iterative Turbo processing. Without such knowledge, linear channel estimators, which treat the interference as white Gaussian noise, provide inaccurate channel estimates and unacceptable error probability with strong interference.

Evidently, an alternative approach for joint channel estimation and interference mitigation is needed. In the absence of interfering pilots, the key is to exploit knowledge of the non-Gaussian statistics of the interference. The problem is basically a compound hypothesis testing problem (averaged over channel uncertainty). Unfortunately, the Maximum Likelihood (ML)

<sup>1</sup>The desired user and the interferer are modeled as independent. In principle, the statistics can be estimated and are not needed *a priori*.

sequence detector becomes computationally impractical since it must search over an exponentially increasing number of combined channel and interference states with block length.

In this paper, we develop an iterative message-passing algorithm for joint channel estimation and interference mitigation, which can also easily incorporate iterative decoding of error-control codes. The algorithm is based on belief propagation (BP), which performs statistical inference on *graphical models* by propagating locally computed “beliefs” [2]. BP has been successfully applied to the decoding of low-density parity-check (LDPC) codes [3], [4]. Other related applications, which have been studied, include combined channel estimation and detection for a single-user fading channel [5]–[7], multiuser detection for CDMA with ideal (nonfading) channels based on a factor graph approach [8] (see also [9], [10]), and the mitigation of multiplicative phase noise in addition to thermal noise [11]–[13]. Unique to this paper is the consideration of fading as well as the presence of a strong interferer. This poses additional challenges, since the desired signal has both phase and amplitude ambiguities, which are combined with the uncertainty associated with the interference.

The following are the main contributions of this paper:

- 1) A factor graph is constructed to describe the model, based on which a BP algorithm is developed. For a finite block of channel uses, the algorithm performs optimal detection and estimation in two passes, one forward and one backward.
- 2) For practical implementation, the belief messages (continuous densities) are parametrized using a small number of variables. The resulting (suboptimal) algorithm has constant complexity per bit (unlike ML which grows exponentially).
- 3) As a benchmark for performance, a lower bound for the optimal error probability is approximated by assuming a genie-aided receiver in which adjacent channel coefficients are revealed.

Numerical results are presented, which show that the message-passing algorithm performs remarkably better than the conventional technique of linear channel estimation followed by detection of individual symbols with or without error-control coding. Furthermore, the relative gain is not substantially diminished in the presence of model mismatch (*i.e.*, the Markov channel model assumed by the receiver is inaccurate), as long as the channels vary relatively slowly.

The remainder of this paper is organized as follows. The system model is formulated in Section II, and Section III develops the message-passing algorithm. A lower bound for the error

probability is studied in Section IV. Simulation results are presented in Section V and conclusions are presented in Section VI.

## II. SYSTEM MODEL

Consider a narrow-band system with a single transmit antenna and  $N_R$  receive antennas, where the received signal at time  $i$  in a frame (or block) of length  $l$  is expressed as

$$\mathbf{y}_i = \mathbf{h}_i x_i + \mathbf{h}'_i x'_i + \mathbf{n}_i \quad i = 1 \dots l \quad (1)$$

where  $x_i$  and  $x'_i$  denote the transmitted symbols of the desired user and interferer, respectively,  $\mathbf{h}_i$  and  $\mathbf{h}'_i$  denote the corresponding  $N_R$ -dimensional vectors of channel coefficients whose covariance matrices are  $\sigma_h^2 \mathbf{I}$  and  $\sigma_{h'}^2 \mathbf{I}$ , and  $\{\mathbf{n}_i\}$  represents the circularly-symmetric complex Gaussian (CSCG) noise at the receiver with covariance matrix  $\sigma_n^2 \mathbf{I}$ . For simplicity, we assume BPSK modulation, *i.e.*,  $x_i, x'_i$  are i.i.d. with values  $\pm 1$ . Here, we first consider an uncoded system and then extend the discussion to coded systems.

Assuming Rayleigh fading,  $\{\mathbf{h}_i\}$  and  $\{\mathbf{h}'_i\}$  are modeled as two independent Gauss-Markov processes, that is, they are generated by first-order auto-regressive relations (e.g., [14]):

$$\mathbf{h}_i = \alpha \mathbf{h}_{i-1} + \sqrt{1 - \alpha^2} \mathbf{w}_i \quad (2a)$$

$$\mathbf{h}'_i = \alpha \mathbf{h}'_{i-1} + \sqrt{1 - \alpha^2} \mathbf{w}'_i \quad (2b)$$

where  $\{\mathbf{w}_i\}$  and  $\{\mathbf{w}'_i\}$  are independent white CSCG processes with covariance  $\sigma_h^2 \mathbf{I}$  and  $\sigma_{h'}^2 \mathbf{I}$ , respectively, and  $\alpha$  determines the correlation between successive fading coefficients. Note that  $\alpha = 0$  corresponds to independent fading, whereas  $\mathbf{h}_i$  and  $\mathbf{h}'_i$  become static if  $\alpha = 1$ , which corresponds to block fading when multiple blocks are considered. Note that (1) also models an OFDM system where  $i$  denotes the index of sub-carriers instead of the time index.

Typically, pilots are inserted periodically between data symbols. For example, 25% pilots refers to pattern “PDDDPDDDPDD...”, where P and D mark pilot and data symbols respectively. Let  $\mathbf{y}_i^j$  denote the sequence  $\mathbf{y}_i, \mathbf{y}_{i+1}, \dots, \mathbf{y}_j$ . The detection problem can be formulated as follows: Given the observations  $\mathbf{y}_1^l$  and the subset of known pilots in  $x_1^l$ , detect the information symbols from the desired user, *i.e.*, the remaining unknown symbols in  $x_1^l$ . Aside from the previous statistical models, knowledge of the channels and interfering symbols are not available.

### III. GRAPHICAL MODEL AND THE MESSAGE-PASSING ALGORITHM

#### A. Graphical Model

An important observation from (1) and (2) is that the fading coefficients  $\{(\mathbf{h}_i, \mathbf{h}'_i)\}_{i=1}^l$  form a Markov chain with state space in  $\mathbb{C}^{2N_r}$ . Also, given  $\{(\mathbf{h}_i, \mathbf{h}'_i)\}_{i=1}^l$ , the input and output variables as a 3-tuple  $(x_i, x'_i, \mathbf{y}_i)$  is independent over times  $i = 1, 2, \dots, l$ . Therefore, the relationships (1) and (2) can be described by the *factor graph* shown in Fig. 1.

Generally, a factor graph is a *bipartite graph*, which consists of two types of nodes: the variable nodes, denoted by a circle in the graph, which represents variables; and the factor nodes, denoted by a square which represents a constraint on the variable nodes connected to it [2], [15]. For example, the node labeled as “ $\mathbf{h}_i, \mathbf{h}'_i$ ” represents the pair of random vectors  $(\mathbf{h}_i, \mathbf{h}'_i)$ . The factor node between nodes  $(\mathbf{h}_i, \mathbf{h}'_i)$  and  $(\mathbf{h}_{i-1}, \mathbf{h}'_{i-1})$  represents the probability constraint specified by (2), which can be obtained from the conditional distribution  $p(\mathbf{h}_i, \mathbf{h}'_i | \mathbf{h}_{i-1}, \mathbf{h}'_{i-1})$ . Similarly, the factor node connecting nodes  $\mathbf{y}_i$ ,  $(\mathbf{h}_i, \mathbf{h}'_i)$  and  $(x_i, x'_i)$  represents the relation given by (1), which is determined by the conditional distribution  $p(\mathbf{y}_i | \mathbf{h}_i, \mathbf{h}'_i, x_i, x'_i)$ . The prior probability distribution of the data symbols is assigned as follows. All BPSK symbols  $x_i$  and  $x'_i$  are uniformly distributed on  $\{-1, 1\}$  except for the subset of pilot symbols in  $x_1^l$ , for which we assume, without loss of generality,  $P\{x_i = 1\} = 1$ . The Markovian property of the graph is that conditioned on any cut node(s), the separated subsets of variables are mutually independent. As we shall see, the Markovian property plays an important role in the development of the message-passing algorithm.

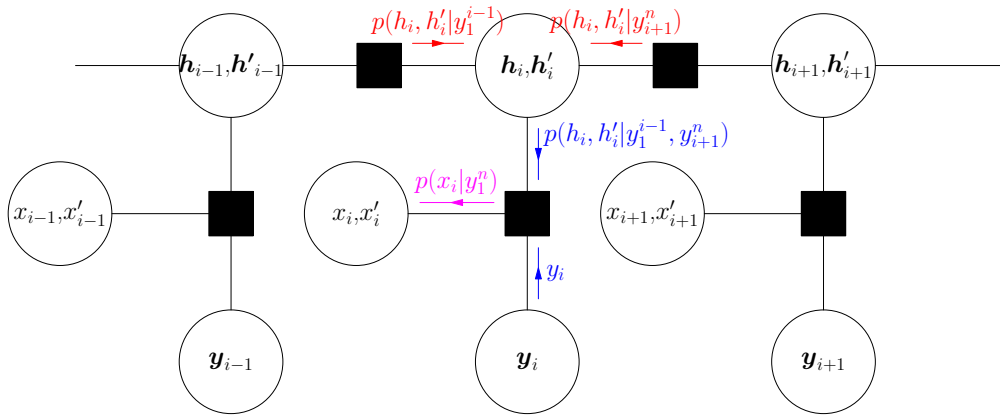


Fig. 1. A factor graph describing the communication system model without channel coding.

Since the graphical model in Fig. 1 fully describes the probability laws of the random variables given by (1) and (2), the detection problem is equivalent to statistical inference on the graph. Simply put, we seek to answer the following question: Given the realization of a subset of the variables on the graph, what can be inferred about the remaining variables?

### B. Exact Inference Via Message Passing

In the problem described in Section II, the goal of inference is to obtain or approximate the marginal posterior probability  $p(x_i|\mathbf{y}_1^l)$ , which is in fact a sufficient statistic of  $\mathbf{y}_i^l$  for  $x_i$ . Problems of such nature have been widely studied (see e.g., [16, Chapter 4] and [2]). In particular, BP is an efficient algorithm for computing the posteriors by iteratively passing messages among neighboring nodes on the graph. In principle, the result of message passing with sufficient iterations gives the exact *a posteriori* probability of each unknown random variable if the factor graph is a tree (*i.e.*, free of cycles) as is the case in the problem considered. For general graphs with cycles, the message-passing algorithm gives approximations of the desired probabilities.

For notational convenience, we assume dual receive antennas ( $N_r = 2$ ) and use the following conventions. Let  $\mathbf{h}_i = [h_{1,i}, h_{2,i}]^T$ ,  $\mathbf{h}'_i = [h'_{1,i}, h'_{2,i}]^T$ ,  $\mathbf{w}_i = [w_{1,i}, w_{2,i}]^T$  and  $\mathbf{w}'_i = [w'_{1,i}, w'_{2,i}]^T$ . Also, letting  $\mathbf{g}_i = [h_{1,i}, h'_{1,i}, h_{2,i}, h'_{2,i}]^T$  and  $\mathbf{u}_i = [w_{1,i}, w'_{1,i}, w_{2,i}, w'_{2,i}]^T$ , the covariance matrix of  $\mathbf{g}_i$  is  $\mathbb{E}[\mathbf{g}_i \mathbf{g}_i^H] = \text{diag}(\sigma_h^2, \sigma_{h'}^2, \sigma_h^2, \sigma_{h'}^2) \triangleq \mathbf{Q}$ . Furthermore, we define

$$\mathbf{Z}_i = \begin{bmatrix} x_i & x'_i & 0 & 0 \\ 0 & 0 & x_i & x'_i \end{bmatrix}$$

With these definitions, (1) and (2) can be rewritten as:

$$\mathbf{y}_i = \mathbf{Z}_i \mathbf{g}_i + \mathbf{n}_i \quad (3)$$

$$\mathbf{g}_i = \alpha \mathbf{g}_{i-1} + \sqrt{1 - \alpha^2} \mathbf{g}_i. \quad (4)$$

Now the goal is to compute for each  $i = 1, \dots, l$ :

$$p(x_i|\mathbf{y}_1^l) = \sum_{x'_i=\pm 1} \int p(\mathbf{Z}_i, \mathbf{g}_i|\mathbf{y}_1^l) d\mathbf{g}_i \propto \sum_{x'_i=\pm 1} \int p(\mathbf{Z}_i, \mathbf{y}_1^{i-1}, \mathbf{y}_i, \mathbf{y}_{i+1}^l, \mathbf{g}_i) d\mathbf{g}_i$$

where the “proportion” notation  $\propto$  indicates that the two sides differ only by a factor which depends only on the observation  $\mathbf{y}_1^l$  (hence has no influence on the decision). For notational simplicity we omit the limits of the integrals, which are over the entire axes of multiple

dimensions in Euclidean space. By the Markovian property,  $(\mathbf{Z}_i, \mathbf{y}_i)$ ,  $\mathbf{y}_1^{i-1}$  and  $\mathbf{y}_{i+1}^l$  are mutually independent given  $\mathbf{g}_i$ . Therefore,

$$\begin{aligned} p(x_i|\mathbf{y}_1^l) &\propto \sum_{x'_i=\pm 1} \int p(\mathbf{y}_i, \mathbf{Z}_i|\mathbf{g}_i) p(\mathbf{y}_1^{i-1}|\mathbf{g}_i) p(\mathbf{y}_{i+1}^l|\mathbf{g}_i) p(\mathbf{g}_i) d\mathbf{g}_i \\ &\propto \sum_{x'_i=\pm 1} \int p(\mathbf{y}_i, \mathbf{Z}_i|\mathbf{g}_i) p(\mathbf{g}_i|\mathbf{y}_1^{i-1}) p(\mathbf{g}_i|\mathbf{y}_{i+1}^l) / p(\mathbf{g}_i) d\mathbf{g}_i. \end{aligned}$$

Since  $\mathbf{Z}_i$  and  $\mathbf{g}_i$  are independent, we finally have

$$p(x_i|\mathbf{y}_1^l) \propto \sum_{x'_i=\pm 1} p(\mathbf{Z}_i) \int p(\mathbf{y}_i|\mathbf{g}_i, \mathbf{Z}_i) p(\mathbf{g}_i|\mathbf{y}_1^{i-1}) p(\mathbf{g}_i|\mathbf{y}_{i+1}^l) / p(\mathbf{g}_i) d\mathbf{g}_i. \quad (5)$$

Note that  $p(\mathbf{y}_i|\mathbf{g}_i, \mathbf{Z}_i)$  is the conditional Gaussian density corresponding to the channel model (1) and  $p(\mathbf{Z}_i) = p(x_i)p(x'_i)$  since the desired symbol and the interference symbol are independent. Also,  $P(x_i = 1) = 1 - P(x_i = -1) = 1$  if the  $i$ th symbol is the pilot for the desired user, otherwise  $P(x_i = 1) = P(x_i = -1) = 1/2$ . Moreover,  $P(x'_i = 1) = P(x'_i = -1) \equiv 1/2$  for all  $i$ , since we do not know the pilot pattern of the interfering user. In order to compute (5), it suffices to compute  $p(\mathbf{g}_i|\mathbf{y}_1^{i-1})$  and  $p(\mathbf{g}_i|\mathbf{y}_{i+1}^l)$ , separately.

We give a brief derivation of the posterior probability  $p(\mathbf{g}_i|\mathbf{y}_1^{i-1})$  below, whereas computation of  $p(\mathbf{g}_i|\mathbf{y}_{i+1}^l)$  is similar by symmetry. The technique is to develop a recursion for the probability. First, we have

$$p(\mathbf{g}_i|\mathbf{y}_1^{i-1}) = \int p(\mathbf{g}_i|\mathbf{g}_{i-1}) p(\mathbf{g}_{i-1}|\mathbf{y}_1^{i-1}) d\mathbf{g}_{i-1}$$

because  $\mathbf{g}_i$  and  $\mathbf{y}_1^{i-1}$  are independent, given  $\mathbf{g}_{i-1}$ . By the Markovian property,  $\mathbf{y}_1^{i-2}$  and  $\mathbf{y}_{i-1}$  are independent given  $\mathbf{g}_{i-1}$ . Therefore,

$$p(\mathbf{g}_i|\mathbf{y}_1^{i-1}) \propto \int p(\mathbf{g}_i|\mathbf{g}_{i-1}) p(\mathbf{y}_{i-1}|\mathbf{g}_{i-1}) p(\mathbf{g}_{i-1}|\mathbf{y}_1^{i-2}) d\mathbf{g}_{i-1}.$$

Since  $\mathbf{g}_{i-1}$  and  $\mathbf{Z}_{i-1}$  are independent,

$$\begin{aligned} p(\mathbf{y}_{i-1}|\mathbf{g}_{i-1}) &= \sum_{\mathbf{Z}_{i-1}} p(\mathbf{y}_{i-1}, \mathbf{Z}_{i-1}|\mathbf{g}_{i-1}) \\ &= \sum_{\mathbf{Z}_{i-1}} p(\mathbf{y}_{i-1}|\mathbf{Z}_{i-1}, \mathbf{g}_{i-1}) p(\mathbf{Z}_{i-1}) \end{aligned}$$

where the summation over  $\mathbf{Z}_{i-1}$  is over all  $(x_{i-1}, x'_{i-1}) = (\pm 1, \pm 1)$ . Therefore, we have

$$p(\mathbf{g}_i|\mathbf{y}_1^{i-1}) \propto \sum_{\mathbf{Z}_{i-1}} \int p(\mathbf{g}_i|\mathbf{g}_{i-1}) p(\mathbf{g}_{i-1}|\mathbf{y}_1^{i-2}) p(\mathbf{y}_{i-1}|\mathbf{g}_{i-1}, \mathbf{Z}_{i-1}) p(\mathbf{Z}_{i-1}) d\mathbf{g}_{i-1}. \quad (6)$$

Note that  $p(\mathbf{g}_i|\mathbf{g}_{i-1})$  is a conditional Gaussian density corresponding to the Gauss-Markov model (2). Therefore, (6) gives a recursion for computing  $p(\mathbf{g}_i|\mathbf{y}_1^{i-1})$  for each  $i = 1, \dots, l$ , which is the essence of the message-passing algorithm. Similarly, we can also derive the inference on  $\mathbf{g}_i$ , which serves as an estimate of channel coefficients at time  $i$ :

$$p(\mathbf{g}_i|\mathbf{y}_1^l) \propto \sum_{\mathbf{Z}_i} p(\mathbf{Z}_i)p(\mathbf{y}_i|\mathbf{g}_i, \mathbf{Z}_i)p(\mathbf{g}_i|\mathbf{y}_1^{i-1})p(\mathbf{g}_i|\mathbf{y}_{i+1}^l)/p(\mathbf{g}_i). \quad (7)$$

In other words, the BP algorithm requires backward and forward message-passing only once in each direction, which is similar to the BCJR algorithm [17]. The key difference between our algorithm and the BCJR is that the Markov chain here has a continuous state space<sup>2</sup>.

The joint channel estimation and interference mitigation algorithm is summarized in Algorithm 1. Basically, the message from a factor node to a variable node is a summary of knowledge about the random variable(s) represented by the variable node based on all observations connected directly or indirectly to the factor node. For example, the message received by node  $(\mathbf{h}_i, \mathbf{h}'_i)$  from the factor node on its left summarizes all information about  $(\mathbf{h}_i, \mathbf{h}'_i)$  based on the observations  $\mathbf{y}_1, \dots, \mathbf{y}_{i-1}$ , which is proportional to  $p(\mathbf{h}_i, \mathbf{h}'_i|\mathbf{y}_1^{i-1})$ . The message from a variable node to a factor node is a summary of information about the variable node based on the observations connected to it. For example, the message passed by node  $(\mathbf{h}_i, \mathbf{h}'_i)$  to the factor node on its left is the inference about  $(\mathbf{h}_i, \mathbf{h}'_i)$  based on the observations  $\mathbf{y}_1, \dots, \mathbf{y}_i$ , *i.e.*,  $p(\mathbf{h}_i, \mathbf{h}'_i|\mathbf{y}_1^i)$ .

### C. Practical Issues

Algorithm 1 cannot be implemented directly using a digital computer because the messages are continuous probability density functions (PDFs). Here we choose to parametrize the PDFs, as opposed to quantizing the PDFs directly. (Simulations not shown here indicate that such a parametrization generally performs better than quantizing the PDFs.)

An observation is that the random variables in Fig. 1 are either Gaussian or discrete. According to (6), it can be shown by induction that the density functions,  $p(\mathbf{g}_i|\mathbf{y}_{i+1}^l)$  and  $p(\mathbf{g}_i|\mathbf{y}_1^{i-1})$  are Gaussian mixtures. Each Gaussian mixture is completely characterized by the amplitudes, means and variances of its constituents. Therefore, we can compute and pass these parameters instead

<sup>2</sup>Another way to derive the message passing algorithm is based on the factor graph, in which the joint probability is factored first and then marginalized to get the associated posterior probability [2].



---

**Algorithm 1** Pseudo code for the message-passing algorithm

---

Initialization:  $P(x'_i = 1) = P(x'_i = -1) = 1/2$  for all  $i$ . The same probabilities are also assigned to  $p(x_i)$  for all  $i$  except for the pilots, for which  $P(x_i = 1) = 1$ . For all  $i$ ,  $p(\mathbf{g}_i)$  is zero mean Gaussian with variance  $\mathbf{Q}$ .

**for**  $i = 1$  to  $l$  **do**

    Compute  $p(\mathbf{g}_i | \mathbf{y}_1^{i-1})$  from (6)

    Compute  $p(\mathbf{g}_i | \mathbf{y}_{i+1}^l)$

**end for**

**for**  $i = 1$  to  $l$  **do**

    Compute  $p(x_i | \mathbf{y}_1^l)$  from (5)

**end for**

---

of PDFs. Let

$$\mathcal{CN}(\mathbf{x}, \mathbf{m}, \mathbf{K}) \equiv \frac{1}{\pi^r \det(\mathbf{K})} \exp(-(\mathbf{x} - \mathbf{m})^H \mathbf{K}^{-1} (\mathbf{x} - \mathbf{m}))$$

where  $\mathbf{m}_{r \times 1}$  and  $\mathbf{K}_{r \times r}$  denote the mean and covariance matrix, respectively. Then we can write  $p(\mathbf{g}_i | \mathbf{g}_{i-1}) = \mathcal{CN}(\mathbf{g}_i, \alpha \mathbf{g}_{i-1}, \sqrt{1 - \alpha^2} \mathbf{Q})$ ,  $p(\mathbf{g}_i) = \mathcal{CN}(\mathbf{g}_i, \mathbf{0}, \mathbf{Q})$  and  $p(\mathbf{y}_i | \mathbf{g}_i, \mathbf{Z}_i) = \mathcal{CN}(\mathbf{y}_i, \mathbf{Z}_i \mathbf{g}_i, \sigma_n^2 \mathbf{I})$ .

Note that the forward recursion (7) starts with a Gaussian density function. According to (6), as the message is passed from node to node, it becomes a mixture of more and more Gaussian densities. Therefore, without loss of generality, we assume that  $p(\mathbf{g}_{i-1} | \mathbf{y}_1^{i-2}) = \sum_j \rho_j \mathcal{CN}(\mathbf{g}_{i-1}, \mathbf{m}_{i-1}^j, \mathbf{K}_{i-1}^j)$ . Substituting into (6), we have after some manipulations

$$p(\mathbf{g}_i | \mathbf{y}_1^{i-1}) \propto \sum_j \sum_{\mathbf{Z}_{i-1}} \rho_j p(\mathbf{Z}_{i-1}) L(j, i) C(j, i) \quad (8)$$

where

$$L(j, i) = \mathcal{CN}(\mathbf{Z}_{i-1} \mathbf{m}_{i-1}^j, \mathbf{y}_{i-1}, \sigma_n^2 \mathbf{I} + \mathbf{Z}_{i-1} \mathbf{K}_{i-1}^j \mathbf{Z}_{i-1}^H) \quad (9)$$

and

$$C(j, i) = \mathcal{CN}(\mathbf{g}_i, \mathbf{m}_i^{j,i}, \mathbf{K}_i^{j,i}) \quad (10)$$

where

$$\mathbf{m}_i^{j,i} = \alpha [\mathbf{m}_{i-1}^j + \mathbf{K}_{i-1}^j \mathbf{Z}_{i-1}^H (\sigma_n^2 \mathbf{I} + \mathbf{Z}_{i-1} \mathbf{K}_{i-1}^j \mathbf{Z}_{i-1}^H)^{-1} (\mathbf{y}_i - \mathbf{Z}_{i-1} \mathbf{m}_{i-1}^j)] \quad (11a)$$

$$\mathbf{K}_i^{j,i} = \alpha^2 \mathbf{K}_{i-1}^j + \sqrt{1 - \alpha^2} \mathbf{Q} - (\alpha \mathbf{K}_{i-1}^j \mathbf{Z}_{i-1}^H) (\sigma_n^2 \mathbf{I} + \mathbf{Z}_{i-1} \mathbf{K}_{i-1}^j \mathbf{Z}_{i-1}^H)^{-1} (\alpha \mathbf{Z}_{i-1} \mathbf{K}_{i-1}^j). \quad (11b)$$

Basically, (8), (9) and (10) give an explicit recursive computation for the amplitude, mean and variance of each Gaussian component in message  $p(\mathbf{g}_i|\mathbf{y}_1^{i-1})$ . Similar computations apply to  $p(\mathbf{g}_i|\mathbf{y}_{i+1}^l)$ .

Examining (11a) and (11b) more closely, ignoring the superscripts, they are the one-step prediction equation and Riccati equations, respectively, for the linear system defined by (3) and (4) with known  $\mathbf{Z}_{i-1}$  [18, Ch.3], [2, Sec. IV.C]. Therefore, passing messages from one end to the other can be viewed as a series of Kalman filters with different weights: In each step, each filter performs the traditional Kalman filter for each hypothesis of  $\mathbf{Z}_{i-1}$  and the filtered result is weighted by the product of the previous weight, the posterior probability of the hypothesis, and  $L(j, i)^3$ .

The preceding Gaussian mixture representation can also be used to compute  $p(\mathbf{g}_i|\mathbf{y}_{i+1}^l)$  and  $p(\mathbf{g}_i|\mathbf{y}_1^l)$ . The number of Gaussian components increases exponentially in the recursive formula (8), which becomes computationally infeasible. In this work, we fix the total number of components and simply pick the components with the largest amplitudes (which correspond to the most likely hypotheses). In general, this problem is equivalent to the problem of survivor-reduction. Two techniques that have been proposed are decision feedback [19] and thresholding [20]. The former limits the maximum number of survivors by assuming the past decisions are correct, while the latter keeps the survivors only when their *a posteriori* probabilities exceed a certain threshold value. According to the preceding analysis, the method we propose falls into the decision feedback category. Obviously, the more components we keep, the better performance we have; however, the higher the complexity at the receiver. We investigate this issue numerically in Section V. A different approach to limiting the number of Gaussian components is presented in [12], [21]–[24]. There the basic idea is to merge components “close” to each other instead of discarding the weakest ones as we do here. However, that requires computing distances between pairs of components, which can lead to significantly higher complexity [22], [24]. The relative performance of these different methods is not clear, and is left for future study.

<sup>3</sup>The value of  $L(j, i)$  is given by (9) and is related to the difference between the filtered result and the new observation.

#### D. Extensions

We have developed the message passing algorithm for a system with dual antennas. However, the approach can be applied to more general scenarios. For example, consider the following multi-antenna system with  $N_R$  antennas at the receiver and  $N_T, N_{T'}$  transmit antennas at the desired and interfering users, respectively:

$$\mathbf{y}_i = \mathbf{H}_i \mathbf{x}_i + \mathbf{H}'_i \mathbf{x}'_i + \mathbf{n}_i \quad (12a)$$

$$\mathbf{H}_i = \mathbf{F} \mathbf{H}_{i-1} + \mathbf{W}_i \quad (12b)$$

$$\mathbf{H}'_i = \mathbf{F}' \mathbf{H}'_{i-1} + \mathbf{W}'_i \quad (12c)$$

where  $\mathbf{y}_i (N_R \times 1)$ ,  $\mathbf{x}_i (N_T \times 1)$ ,  $\mathbf{x}'_i (N_{T'} \times 1)$  are the received signal, desired user's signal and interfering signal, respectively, at time  $i$ ,  $\mathbf{n}_i (N_R \times 1)$  is a CSCG noise, and  $\mathbf{H}_i (N_R \times N_T)$  and  $\mathbf{H}'_i (N_R \times N_{T'})$  are channel matrices, which are mutually independent. Equations (12b) and (12c) represent the evolution of the channels, where  $\mathbf{F}$  and  $\mathbf{F}'$  are square matrices (instead of scalars), and  $\mathbf{W}_i$  and  $\mathbf{W}'_i$  are independent CSCG noises.

Let  $\mathbf{h}_{j,i}$  represent the  $j$ th row of  $\mathbf{H}_i$ , and define

$$\mathbf{g}_i = [\mathbf{h}_{1,i}, \mathbf{h}'_{1,i}, \mathbf{h}_{2,i}, \mathbf{h}'_{2,i}, \dots, \mathbf{h}_{N_R,i}, \mathbf{h}'_{N_R,i}]^T \quad (13a)$$

$$\mathbf{u}_i = [\mathbf{w}_{1,i}, \mathbf{w}'_{1,i}, \mathbf{w}_{2,i}, \mathbf{w}'_{2,i}, \dots, \mathbf{w}_{N_R,i}, \mathbf{w}'_{N_R,i}]^T \quad (13b)$$

$$\mathbf{Z}_i = \mathbf{I}_{N_R} \otimes [\mathbf{x}_i^T, \mathbf{x}'_i^T] \quad (13c)$$

$$\mathbf{A} = \mathbb{E}[\mathbf{g}_i \mathbf{g}_{i-1}^H] (\mathbb{E}[\mathbf{g}_{i-1} \mathbf{g}_{i-1}^H])^{-1} \quad (13d)$$

$$\mathbf{B} = \mathbb{E}[\mathbf{g}_i \mathbf{u}_i^H] \quad (13e)$$

where  $\otimes$  represents the Kronecker product and  $\mathbf{I}_{N_R}$  represents the  $N_R \times N_R$  identity matrix. Note that (3) and (4) are still valid, when  $\alpha$  and  $\sqrt{1 - \alpha^2} \mathbf{Q}$  are replaced by  $\mathbf{A}$  and  $\mathbf{B}$ , respectively. Therefore, with this replacement, the BP algorithm for this general model remains the same.

We can also replace the Gauss-Markov model with higher order Markov models. By expanding the state space (denoted by  $\mathbf{S}_i$ ), we can still construct the corresponding factor graph by replacing variable nodes ( $\mathbf{H}_i, \mathbf{H}'_i$ ) with  $\mathbf{S}_i$ , and a similar algorithm can be derived as before. Also, extensions to systems with more than one interference can be similarly derived.

Furthermore, the proposed scheme can in principle be generalized to any signal constellation and any space-time codes, including QPSK, 8-PSK, 16-QAM and Alamouti codes. However, as

the constellation size, the codebook size or the number of interferers increases, the complexity of the algorithm increases rapidly, while the advantage over linear channel estimation vanishes because the interference becomes more Gaussian. Thus the algorithm proposed in this paper is particularly suitable for BPSK and QPSK modulations, space-time codewords with short block length and a small number of interferers.

### E. Complexity

Suppose that there are  $m$  channel coefficients, hence  $\mathbf{g}$  is a vector of length  $m$ , the number of receiver antennas is  $N_R$ , the maximum number of Gaussian components we allow is  $C$ , and the size of alphabet of  $\mathbf{Z}_i$  is  $|\mathcal{A}|$ . The complexity of computing  $p(\mathbf{g}_i|\mathbf{y}_1^{i-1})$  is then  $O(C|\mathcal{A}|N_R^2l)$ , where  $N_R^2$  is due to the matrix inverse in (11b). Similar complexity is needed to compute  $p(\mathbf{g}_i|\mathbf{y}_{i+1}^l)$ . To synthesize the results from the backward and forward message passing via (5), we need  $O(C^2|\mathcal{A}|m^2l)$  computations, where  $m^2$  is again due to the matrix inverse. Thus, the total complexity is  $O((CN_R^2 + C^2m^2)|\mathcal{A}|l)$ , *i.e.*, the complexity is linear in the frame length and quadratic in the number of receiver antennas (*i.e.*, constant per bit) and the total number of channel coefficients. To reduce the complexity, one can reduce  $C$ , which causes performance loss. One can also try to approximate the matrix inverse (or equivalently, replace the Kalman filter with a suboptimal filter). However, this replacement raises two issues, which we do not address here: (i) How to assign weights to each filter (as in (9)), and (ii) How to efficiently compute the backward and forward results (*i.e.*, without directly inverting the covariance matrices).

### F. Integration with Channel Coding

Channel codes based on factor graphs can be easily included within the message-passing framework developed so far. This is illustrated in Fig. 2, which shows a sparse graphical code added to the factor graph for the model (1) and (2).

The larger factor graph is no longer acyclic. Therefore, the message-passing algorithm is not optimal for this graph even if one could keep all detection hypotheses (*i.e.*, the number of mixture components is unrestrained). Based on the factor graph, one can develop many message-passing schedules. To exploit the slow variation of the fading channel, the non-Gaussian property of the interfering signal and the structure of graphical codes, a simple idea is to allow the detector and decoder to exchange their extrinsic information (EI). For example, suppose that at

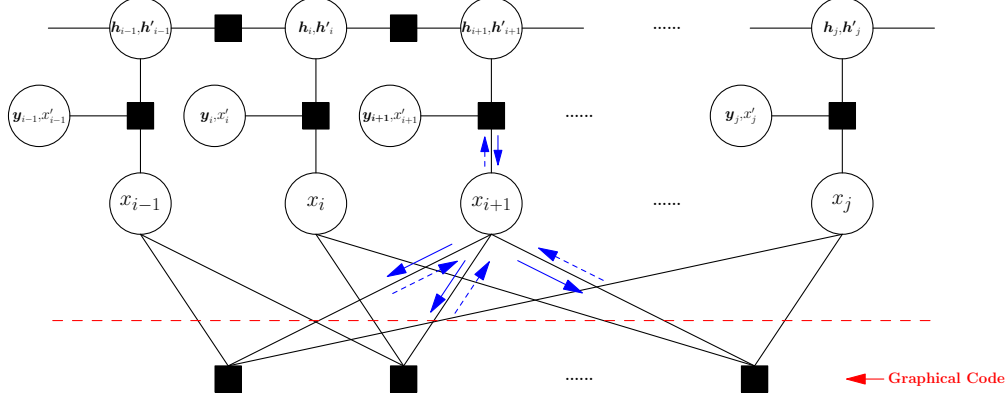


Fig. 2. A factor graph for joint detection, estimation and decoding. The solid arrows show EI passed from the detector to the decoder, and the dashed arrows show EI passed from the decoder to the detector.

a certain message-passing stage, the node  $x_{i+1}$  computes its *a posteriori* probability (APP) from the detector. Then the node  $x_{i+1}$  can distribute the EI (which is obtained by removing the posterior probability of  $x_{i+1}$  in the APP) to the sub-graph of the graphical code, which is described by the solid arrows in Fig. 2. After  $x_{i+1}$  collects the “beliefs” from all its edges, it passes the EI (which is obtained by multiplying together all “beliefs” but the one coming from the detector) back to the detector. This process is described by the dashed arrows in Fig. 2. In other words, both the detector and the decoder compute their posterior probabilities from received EI.

In this paper, we use LDPC codes with the following simple strategy: We run the detection part as before and then feed the EI to the LDPC decoder through variable nodes  $x_i$ . After running the LDPC decoder several rounds, we feed back the extrinsic information to the detection sub-graph. Let  $I_{det}$  denote the total number of EI exchanges between decoder and detector, and  $I_{dec}$  denote the number of iterations of the LDPC decoder during each EI exchange. For a fixed total number of LDPC iterations  $I_{det} \times I_{dec}$ , we will investigate how these two parameters impact the performance in Section V.

### G. Alternative Factor Graphs

We remark that the design of factor graphs is not unique. Unlike most other work (including [11]–[13]), where each random variable is made a variable node, the factor graph in Fig. 1 consists of nodes representing multiple variables so that the graph is free of cycles. This was chosen because message-passing does not perform exact inference on the *cyclic* graph consisting of only

single-variable nodes. In fact numerical experiments (omitted here) show significant performance degradation due to the large number of short cycles if each variable is made a separate node (e.g., the cycle through  $\mathbf{h}_i, \mathbf{h}'_i, \mathbf{h}_{i+1}, \mathbf{h}'_{i+1}$ ). We also note that even though the use of LDPC codes introduce cycles (see Fig. 2), the degree of such cycles are typically quite large. Hence message-passing performs very well.

#### IV. ERROR FLOOR DUE TO CHANNEL UNCERTAINTY

We note that the bit-error rate (BER) of the uncoded system does not vanish even in absence of noise. To see this, consider a genie-aided receiver by revealing both  $(\mathbf{h}_{i-1}, \mathbf{h}'_{i-1})$  and  $(\mathbf{h}_{i+1}, \mathbf{h}'_{i+1})$  when detecting symbol  $x_i$ . Even in absence of noise, there remains channel uncertainty, which contributes estimation error, which, in turn, causes non-negligible error probability.

In fact, the genie-aided receiver gives a lower bound on error probability for the exact message passing algorithm. In this section, we derive an approximation to this lower bound. Numerical results in Section V indicate that the difference between the approximate lower bound and the actual genie-aided performance is small.

Consider the error probability of jointly detecting  $[x_i, x'_i]$  with the help of the genie. Let  $\mathbf{h}_i = \hat{\mathbf{h}}_i + \tilde{\mathbf{h}}_i$  and  $\mathbf{h}'_i = \hat{\mathbf{h}}'_i + \tilde{\mathbf{h}}'_i$  where  $\hat{\mathbf{h}}_i$  and  $\hat{\mathbf{h}}'_i$  are the estimates of  $\mathbf{h}_i$  and  $\mathbf{h}'_i$ , respectively, and  $\tilde{\mathbf{h}}_i$  and  $\tilde{\mathbf{h}}'_i$  are the respective estimation errors. Then the channel model can be rewritten as

$$\mathbf{y}_i = \hat{\mathbf{h}}_i x_i + \hat{\mathbf{h}}'_i x'_i + \tilde{\mathbf{n}}_i$$

where  $\tilde{\mathbf{n}}_i$  is white Gaussian noise with variance matrix  $\sigma_n^2 \mathbf{I} = \left( \frac{1-\alpha^2}{1+\alpha^2} (\sigma_h^2 + \sigma_{h'}^2) + \sigma_n^2 \right) \mathbf{I}$ .

Let  $\hat{x}_i$  and  $\hat{x}'_i$  be the estimates of  $x_i$  and  $x'_i$ , respectively. Define the two events:  $E_1 = \{\hat{x}_i \neq x_i \text{ and } \hat{x}'_i = x'_i\}$  and  $E_2 = \{\hat{x}_i \neq x_i \text{ and } \hat{x}'_i \neq x'_i\}$ . Following a standard analysis [25, App. A], we have

$$\begin{aligned} P(\text{error}) &= P(\{\hat{x}_i \neq x_i \text{ and } \hat{x}'_i = x'_i\}) + P(\{\hat{x}_i \neq x_i \text{ and } \hat{x}'_i \neq x'_i\}) \\ &= \left( \frac{1-\mu_1}{2} \right)^2 (2 + \mu_1) + \left( \frac{1-\mu_2}{2} \right)^2 (2 + \mu_2) \end{aligned} \quad (14)$$

where

$$\begin{aligned} \mu_1 &= \sqrt{\frac{\alpha^2 \sigma_h^2}{\alpha^2 \sigma_h^2 + (1 + \alpha^2) \sigma_n^2}} \\ \mu_2 &= \sqrt{\frac{\alpha^2 (\sigma_h^2 + \sigma_{h'}^2)}{\alpha^2 (\sigma_h^2 + \sigma_{h'}^2) + (1 + \alpha^2) \sigma_n^2}} \end{aligned}$$

We remark that the existence of an error floor is inherent to the channel model. Despite its simplicity, the channel cannot be tracked exactly based on pilots.

## V. SIMULATION RESULTS

In this section, the model presented in Section II, *i.e.*, the dual-receive-antenna system with BPSK signaling, is used for simulation. The performance of the message-passing algorithm is plotted versus signal-to-noise ratio  $SNR = \sigma_h^2/\sigma_n^2$ , where the covariance matrix of the noise is  $\sigma_n^2 \mathbf{I}$ . We set  $\alpha = .99$  and limit the maximum number of Gaussian components to 8. Within each block, there is one pilot in every 4 symbols. For the uncoded system, we set the frame length  $l = 200$ . For the coded system, we use a (500, 250) irregular LDPC code and multiplex one LDPC codeword into a single frame, *i.e.*, we do not code across multiple frames.

### A. Performance of Uncoded System

1) *BER Performance*: Results for the message-passing algorithm with the Gaussian mixture messages described in Section III are shown in Figs. 3 to 7. We also show the performance of three other receivers for comparison. The first is denoted by “MMSE”, which estimates the desired channel by taking a linear combination of adjacent received value. This MMSE estimator treats the interference as white Gaussian noise. The second is the genie-aided receiver described in Section IV, denoted by “Genie-Aided Scheme”, which gives a lower bound on the performance of the message-passing algorithm. The third one is denoted by “ML with full CSI”, which performs maximum likelihood (ML) detection for each symbol assuming that the realization of the fading processes is revealed to the detector by a genie, which lower bounds the performance of all other receivers. We also plot the approximation of the BER for the optimal genie-aided receiver obtained from (14) using a dashed line.

Fig. 3 shows uncoded BER vs. SNR, where the power of the interference is 10 dB weaker, 3 dB weaker and equal to that of the desired user, respectively. The message-passing algorithm generally gives a significant performance gain over the MMSE channel estimator, especially in the high SNR region. Note that thermal noise dominates when the interference is weak. Therefore, relatively little performance gain over the MMSE algorithm is observed in Fig. 3(a). In the very low SNR region, the MMSE algorithm slightly outperforms the message-passing algorithm, which is probably due to the limitation on number of Gaussian components.

The trend of the numerical results shows that the message-passing algorithm effectively mitigates or partially cancels the interference at all SNRs of interest, as opposed to suppressing it by linear filtering. We see that there is still a gap between the performance of the message-passing algorithm and that of the genie-aided receiver. The reason is that revealing both  $\mathbf{h}$  and  $\mathbf{h}'$  enables receiver to detect the symbol of the interferer with improved accuracy. However, without the genie, even the optimal detector cannot accurately estimate the interfering symbol. Another observation is that the analytical estimate is closer to the message-passing algorithm performance with stronger interference.

2) *Channel Estimation Performance:* The channel estimate from the message-passing algorithm is much more accurate than that from the conventional linear channel estimation. Consider, for example, the situation where the interference signal is 3 dB weaker than the desired signal. Suppose one pilot is used after every three data symbols. The simulated mean squared error for the channel estimate from the message-passing algorithm is equal to  $5.495 \times 10^{-2}$ ,  $2.630 \times 10^{-2}$  and  $1.660 \times 10^{-2}$  at SNRs of 10, 15 and 20 dB, respectively. The corresponding mean square error from linear estimation is equal to 0.112, 0.105 and 0.102. Note that the performance of the linear estimator hardly improves as the SNR increases because the signal-to-interference-and-noise ratio is no better than 3 dB regardless of the SNR. This is the underlying reason for the poor performance of the linear receiver shown in Fig. 3.

### B. Performance of Coded System

Consider coded transmission using a (500, 250) irregular LDPC code and with one LDPC code word in each frame, *i.e.*, no coding across multiple frames. Since we insert one pilot every 3 symbols, the total frame length is 667 symbols. For the message-passing algorithm, we present the performance of two message-passing schedules: (a)  $I_{det} = 1$  and  $I_{dec} = 50$  denoted by “Separate Message-passing Alg.”, *i.e.*, the receiver detects the symbol first, then passes the likelihood ratio to the LDPC decoder without any further EI exchanges (separate detection and decoding), and (b)  $I_{det} = 5$  and  $I_{dec} = 10$ , denoted by “Joint Message-passing Alg.”, *i.e.*, there are five EI exchanges and the LDPC decoder iterates 10 rounds in between each EI exchange. For the other two receiver algorithms, the total number of iterations of LDPC decoder are both 50. As shown in Fig. 4, the message-passing algorithm preserves a significant advantage over the traditional linear MMSE algorithm and the joint message-passing algorithm gains even more.



The performance of the joint algorithm with different parameters will be investigated further in the next subsection.

### C. Performance Impact of Parameters

1) *Impact of Mixture Gaussian Approximation:* As previously mentioned, the number of Gaussian components in the messages related to the fading coefficients grows exponentially. For implementation, we often have to truncate or approximate the mixture Gaussian message. In this paper, we keep only a fixed number of components with the maximum amplitudes. The maximum number of components clearly has some impact on the performance. Here we present some numerical experiments to illustrate this effect.

When the pilot density is high, say 50%, there is no need to keep many Gaussian components in each message. In fact, keeping two components is essentially enough. However, when the pilot density is lower, say 25%, the situation is different. Fig. 5 shows the BER performance when we keep different numbers of Gaussian components in the message-passing algorithm where the pilot density is 25%. For this case, we need 8 components for each message passing step. Indeed, the lower the pilot density, the more Gaussian components we need to achieve the same performance. When the pilot density is low, we must keep a sufficient number of components, corresponding to a sufficient resolution for the message. Roughly speaking, the number of Gaussian components needed is closely related to the number of hypotheses arising from symbols between the symbol of interest and the nearest pilot.

2) *Impact of Imperfect Channel Statistical Knowledge:* Although the statistical model for the channel is usually determined *a priori*, the parameters of the model are often based on on-line estimates, which may be inaccurate. The following simulations evaluate the robustness of the receiver when some parameters, or the model itself is not accurate. The simulation conditions here are the same as for the previous uncoded system with 3 dB weaker interference. Fig. 6(a) plots the BER performance against the correlation coefficient  $\hat{\alpha}$  assumed by the receiver, which may not be equal to the actual correlation coefficient  $\alpha$  for the Gauss-Markov model. It is clear that the mismatch in  $\alpha$  does not cause much degradation. Furthermore, we observe that it is generally better to overestimate the coefficient than to underestimate it. The result of a similar experiment is plotted in Fig. 6(b), where the receiver assumes the Gauss-Markov model, while

the actual channels follow the Clarke model [25, Ch. 2].<sup>4</sup> We see that the message-passing algorithm still works well. In fact, as long as the channel varies relatively slowly, modeling it as a Gauss-Markov process leads to good performance.

3) *Impact of Message Passing Scheduling:* For the coded system the performance will be affected by the message-passing schedule. Here different schedules correspond to the different values of  $I_{det}$  and  $I_{dec}$ . Using the setup for the previous coded-system simulation, results for various values of  $I_{det}$  and  $I_{dec}$  are compared in Fig. 7. Generally speaking, if  $I_{dec}$  or  $I_{det} \times I_{dec}$  is fixed, more EI exchanges lead to better performance. We also observe that when  $I_{dec}$  is relatively large, say 30, the performance gain from EI exchanges is small. The reason is that when  $I_{dec}$  is large, the output of the LDPC decoder “hardens”, *i.e.*, the decoder essentially decides what each information bit is. When the EI is passed to the detector, all symbols look like pilots from the point of view of the detector. Therefore, there is not much gain in this case.

## VI. CONCLUSION

We have studied a message-passing algorithm for joint channel estimation, interference mitigation and decoding based on graphical models and BP. For the scenarios considered, the message-passing algorithm provides a much lower error floor than linear channel estimation. The results with coding show at least 5 dB gain at relatively high SNRs. Also, this gain is robust with respect to a mismatch in channel statistics.

We have considered only two users with dual receive antennas. Although this is an important case, and the approach can be generalized, there may be implementation (complexity) issues with extending the algorithm. For example, if we have more than one interferer or use larger constellations, the number of hypotheses at each message-passing step increases significantly. To maintain a target performance, we need to increase the number of Gaussian components in each step accordingly. Therefore, the complexity may significantly increase with these extensions. Finally, the algorithm is difficult to analyze. While our results give some basic insights into performance, relative gains are difficult to predict.

Directions for future work include extensions to MIMO channels (where channel modeling within the message-passing framework becomes a challenge) as well as implementation issues including methods for reducing complexity.

<sup>4</sup>We set  $\hat{\alpha}$  according to the auto-correlation function for the Clark model.

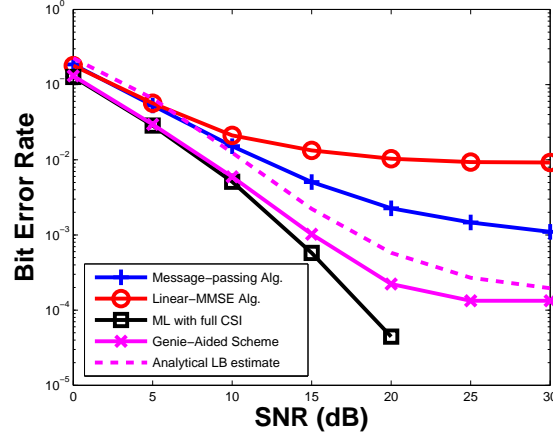
## ACKNOWLEDGMENT

The authors would like to thank Mingguang Xu for constructive discussions and help with the simulations.

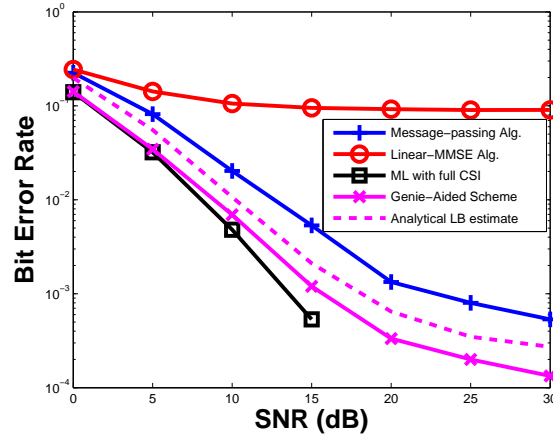
## REFERENCES

- [1] K. Sil, M. Agarwal, D. Guo, and M. L. Honig, "Performance of Turbo decision-feedback detection and decoding in downlink OFDM," in *IEEE Wireless Commun. & Networking Conf.*, Mar. 2007.
- [2] F. R. Kschischang, B. J. Frey, and H.-A. Loeliger, "Factor graphs and the sum-product algorithm," *IEEE Trans. Inf. Theory*, vol. 47, no. 2, pp. 498–519, Feb. 2001.
- [3] T. J. Richardson and R. L. Urbanke, "The capacity of low-density parity-check codes under message-passing decoding," *IEEE Trans. Inf. Theory*, vol. 47, no. 2, pp. 599–618, Feb. 2001.
- [4] T. J. Richardson, M. A. Shokrollahi, and R. L. Urbanke, "Design of capacity-approaching irregular low-density parity-check codes," *IEEE Trans. Inf. Theory*, vol. 47, no. 2, pp. 619–637, Feb. 2001.
- [5] A. P. Worthen and W. Stark, "Unified design of iterative receivers using factor graphs," *IEEE Trans. Inf. Theory*, vol. 47, no. 2, pp. 843–849, Feb. 2001.
- [6] X. Jin, A. W. Eckford, and T. E. Fuja, "LDPC codes for non-coherent block fading channels with correlation: Analysis and design," *IEEE Trans. Commun.*, vol. 56, no. 1, pp. 70–80, Jan. 2008.
- [7] C. Komninakis and R. D. Wesel, "Joint iterative channel estimation and decoding in flat correlated Rayleigh fading," *IEEE J. Sel. Areas Commun.*, vol. 19, no. 9, pp. 1706–1717, Sep. 2001.
- [8] J. Boutros and G. Caire, "Iterative multiuser joint decoding: Unified framework and asymptotic analysis," *IEEE Trans. Inf. Theory*, vol. 48, no. 7, pp. 1772–1793, Jul. 2002.
- [9] D. Guo and T. Tanaka, "Generic multiuser detection and statistical physics," in *Advances in Multiuser Detection*, M. Honig, Ed. John Wiley & Sons Inc., 2008, to appear.
- [10] D. Guo and C.-C. Wang, "Multiuser detection of sparsely spread CDMA," *IEEE J. Sel. Areas Commun.*, vol. 26, no. 4, pp. 421–431, Apr. 2008.
- [11] A. Barbieri, G. Colavolpe, and G. Caire, "Joint iterative detection and decoding in the presence of phase noise and frequency offset," *IEEE Trans. Commun.*, vol. 55, no. 1, pp. 171–179, Jan. 2007.
- [12] G. Colavolpe, A. Barbieri, and G. Caire, "Algorithms for iterative decoding in the presence of strong phase noise," *IEEE J. Sel. Areas Commun.*, vol. 23, no. 9, pp. 1748–1757, Sep. 2005.
- [13] J. Dauwels and H. Loeliger, "Phase estimation by message passing," in *Communications, IEEE International Conference on*, Paris, France, Jun. 2004, pp. 523–527.
- [14] I. Abou-Faycal, M. Médard, and U. Madhow, "Binary adaptive coded pilot symbol assisted modulation over Rayleigh fading channels without feedback," *IEEE Trans. Commun.*, vol. 53, no. 6, pp. 1036–1046, June 2005.
- [15] H.-A. Loeliger, J. Dauwels, J. Hu, S. Korl, L. Ping, and F. R. Kschischang, "The factor graph approach to model-based signal processing," *Proceedings of the IEEE*, vol. 95, no. 6, pp. 1295–1322, Jun 2007.
- [16] D. C. MacKay, *Information Theory, Inference and Learning Algorithm*. Cambridge University Press, 2003.
- [17] L. R. Bahl, J. Cocke, F. Jelinek, and J. Raviv, "Optimal decoding of linear codes for minimizing symbol error rate," *IEEE Trans. Inf. Theory*, vol. 20, no. 2, pp. 284–287, 1974.
- [18] B. D. Anderson and J. B. Moore, *Optimal Filtering*. Dover Publications, Inc., 1979.

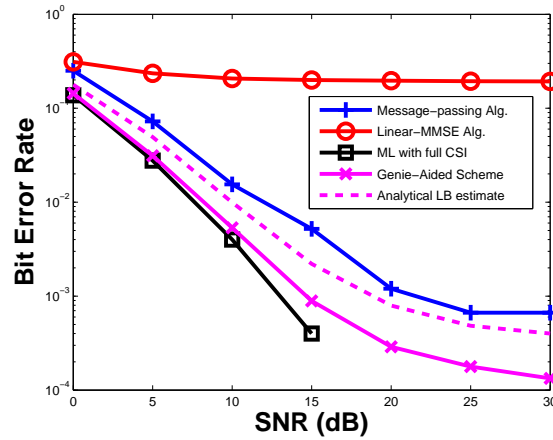
- [19] S. J. Simmons, “Breadth-first trellis decoding with adaptive effort,” *IEEE Trans. Commun.*, vol. 38, no. 1, pp. 3–12, Jan. 1990.
- [20] Q. Dai and E. Shwedyk, “Detection of bandlimited signals over frequency selective Rayleigh fading channels,” *IEEE Trans. Commun.*, vol. 42, no. 2/3/4, pp. 941–950, Feb./Mar./Apr. 1994.
- [21] J. Dauwels, S. Korl, and H.-A. Loeliger, “Particle methods as message passing,” in *Information Theory, IEEE International Symposium on*, Jul 2006, pp. 2052–2056.
- [22] D. W. Scoot and W. F. Szewczyk, “From kernels to mixtures,” *Technometrics*, vol. 43, no. 3, pp. 323–335, August 2001.
- [23] E. B. Sudderth, A. T. Ihler, W. T. Freeman, and A. S. Willsky, “Nonparametric belief propagation,” in *Computer Vision and Pattern Recognition, IEEE Conference on*, vol. 1, June 2003, pp. 605–612.
- [24] B. Kurkoski and J. Dauwels, “Message-passing decoding of lattices using Gaussian mixtures,” in *Information Theory, IEEE International Symposium on*, 2008, pp. 2489–2493.
- [25] D. Tse and P. Viswanath, *Fundamentals of Wireless Communications*. Cambridge University Press, 2005.



(a)



(b)



(c)

Fig. 3. The BER performance of the message-passing algorithm. The density of pilots is 25%. (a) The power of the interference is 10 dB weaker than that of the desired user. (b) The power of the interference is 3 dB weaker. (c) The power of the interference is identical to that of the desired user.

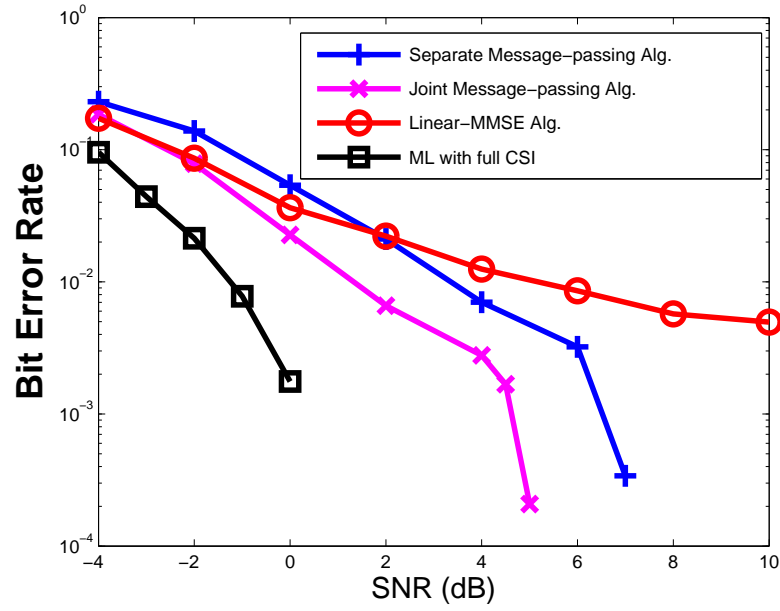


Fig. 4. BER performance for the system with a  $(500, 250)$  irregular LDPC code. The interference is 3 dB weaker than the desired signal. The density of pilots is 25%.

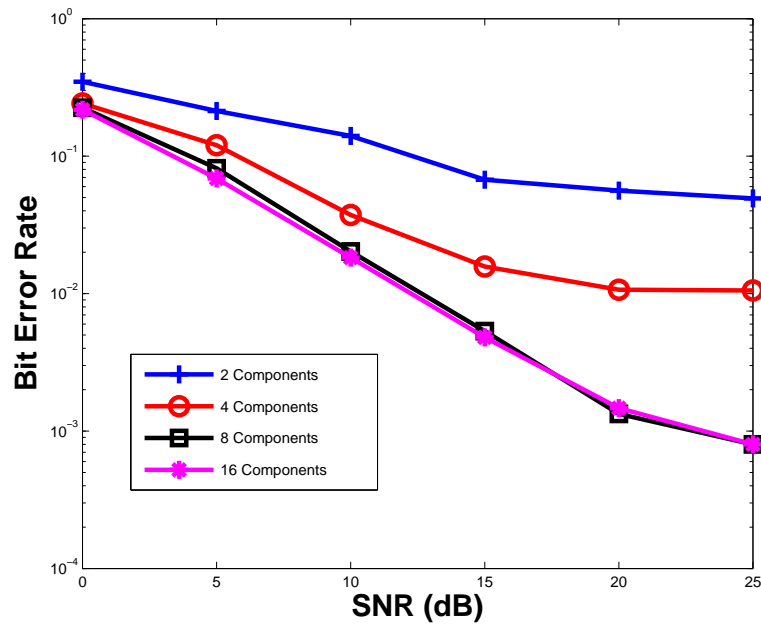


Fig. 5. The BER performance with different number of components in the messages. The interference is assumed to be 3 dB weaker than the desired signal. The density of pilots is 25%.

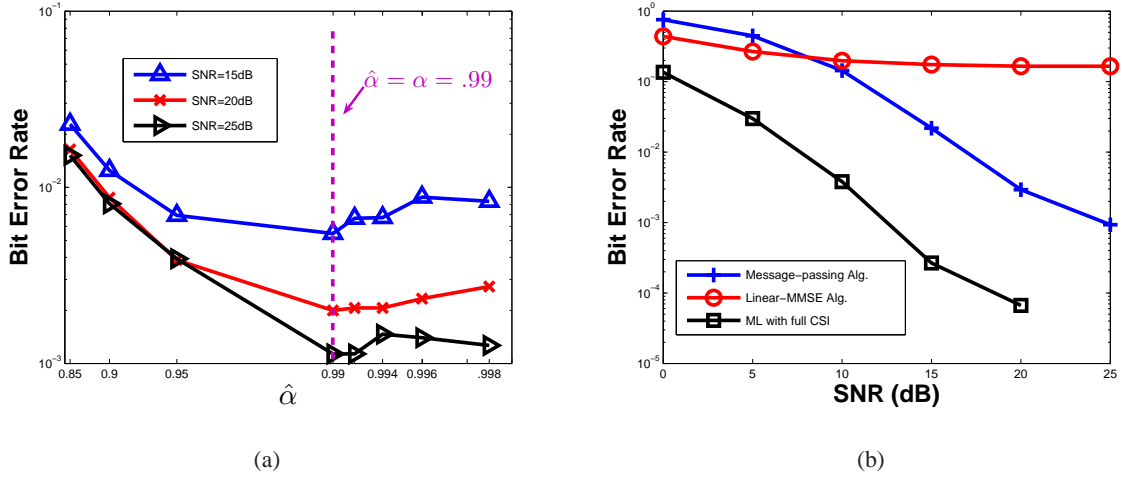


Fig. 6. The BER performance with channel mismatch. (a) Performance with inaccurate channel correlation coefficient  $\alpha$ , and with 3 dB weaker interference. (b) Performance with the Clarke channel with normalized maximum Doppler frequency 0.02 and 3 dB weaker interference.

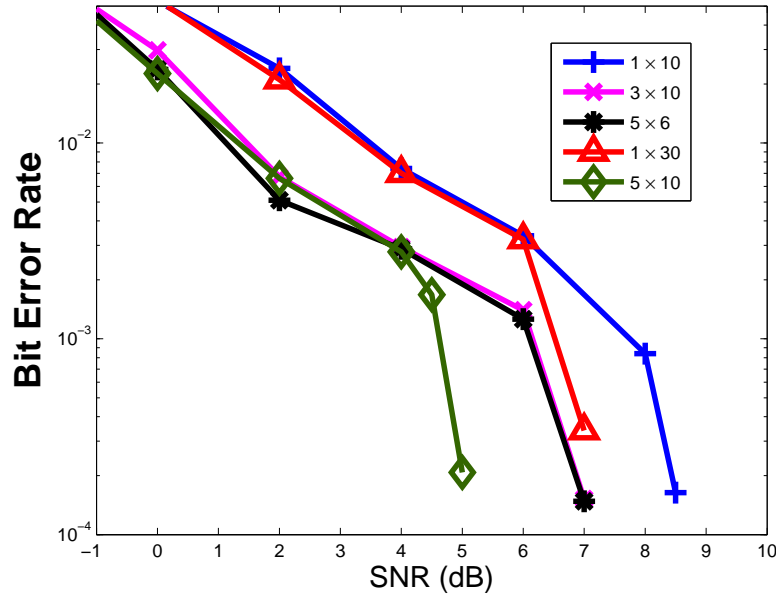


Fig. 7. The impact of different message-passing schedules.